Photochemical & Photobiological Sciences

PAPER

View Article Online
View Journal | View Issue

Cite this: *Photochem. Photobiol. Sci.*, 2018, **17**, 822

β-Diketone derivatives: influence of the chelating group on the photophysical and mechanofluorochromic properties†

Marine Louis,[a] Régis Guillot,[b] Rémi Métivier *[a] and Clémence Allain *[a]

Received 15th February 2018,
Accepted 3rd May 2018

DOI: 10.1039/c8pp00070k

rsc.li/pps

A diphenyl-boron β-diketonate complex was synthesized. Its photophysical properties were studied in solution and in the solid-state, and compared to those of its parent diketone and the corresponding difluoro-boron complex. TD-DFT calculations show that the molecular orbitals involved in the first Franck–Condon transition are very different for the three compounds studied. The difluoro-boron complex is strongly fluorescent in solution, and remains fluorescent in the solid-state. The free diketone turns to be very weakly fluorescent in solution and displays significant Aggregation Induced Enhanced Emission (AIEE) in the crystalline state, which can be explained by a rigidification of the molecule, while the diphenyl-boron complex is weakly fluorescent in solution as well as in the solid-state. For the free diketone and the difluoro-boron complex a mechanofluorochromic response is observed upon grinding the crystalline powder in a mortar, while for the diphenyl-boron complex no fluorescence emission change is detected under these conditions. Overall, this study shows that the nature of the chelating group has a crucial influence on the photophysical and mechanofluorochromic properties of β-diketonate complexes, leading to a wide variety of behaviors within the closely related structures of such derivatives.

Introduction

The development of compounds fluorescent in the solid state is currently a topic of high interest, both for elucidating the mechanisms responsible for the fluorescence changes observed when going from the solution to the solid-state, and for various applications, such as sensors or emissive displays. Among the solid-state fluorescent materials, mechanofluorochromic materials are those for which fluorescence emission changes upon application of a mechanical stress (pressure, shearing).[1] The study of these mechanofluorochromic materials is rapidly developing, with potential applications as force sensors or in security technologies, and several mechanofluorochromic systems have been described during the past five years including coordination complexes,[2] organic dyes,[3] and polymers.[4]

Since the first description of their mechanofluorochromism by Fraser *et al.* in 2010,[5] difluoroboron β-diketonate (DFB) complexes have been widely studied since they possess appealing properties such as versatile synthesis, high fluorescence quantum yields in the solid state, large fluorescence emission shifts upon mechanical stimulation, and a substituent-dependent backward reaction to the original fluorescence emission after mechanical stimulation.[6] As a consequence, numerous derivatives belonging to this family have been described, such as dibenzoylmethane systems with different substituents on the phenyl rings,[7–9] or diketones substituted with larger aromatic rings[10,11] or heterocycles.[12]

However, the studies aiming at deciphering the influence of the boron chelating group on the photophysical properties of these complexes are more scarce. Comparison between free diketones and their boron difluoride complexes has been made on dinaphthoylmethane diketones, in which the complexation induces an enhancement of the fluorescence emission both in solution and in the solid state[11] and on azepane substituted dibenzoyl β-diketones in which the complexation induces a loss of fluorescence emission in solution.[13] The β-diketones described in the references cited above display Aggregation Induced Emission (AIE) or Aggregation Induced Enhanced Emission (AIEE) and are in most cases mechanofluorochromic. Interestingly, a dibenzoyl β-diketone bearing a dimethylamino group in the *para* position of one of the phenyl rings has been studied separately as a free ligand,[14] as

[a]*PPSM, ENS Cachan, CNRS, Université Paris-Saclay, 94235 Cachan, France.. E-mail: callain@ppsm.ens-cachan.fr, metivier@ppsm.ens-cachan.fr*
[b]*ICMMO, Université Paris-Sud, CNRS, Université Paris-Saclay, 91405 Orsay, France*

†Electronic supplementary information (ESI) available: NMR spectra, crystallographic data. CCDC 1823426. For ESI and crystallographic data in CIF or other electronic format see DOI: 10.1039/c8pp00070k

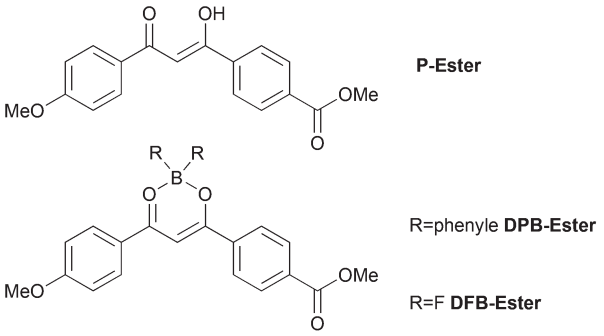

Fig. 1 Structures of β-diketone **P-Ester** studied, together with those of its boron complexes **DPB-Ester** and **DFB-Ester**.

difluoroboron and di-(pentafluorophenyl) complexes[15] and as a diphenyl-boron complex.[16] It is worth noting that this diphenyl-boron complex is described as mechanofluorochromic, with a distinct response to distinct forces, which is promising for the development of force sensors.

Based on these data, modifying the boron chelating group of β-diketonate complexes appears as an interesting and straightforward strategy from the point of view of organic synthesis leading to new mechanofluorochromic compounds with distinct properties. We decided to prepare an original diphenyl-boron-β-diketone complex substituted with methoxy and ester groups (**DPB-Ester**, Fig. 1) and compare its photophysical properties, in solution and in the solid state, with those of its corresponding metal-free diketone precursor (**P-Ester**) and its corresponding difluoroboron complex (**DFB-Ester**).[17]

Experimental

Synthetic procedures

All chemicals were of reagent grade and used without further purification. Anhydrous solvents were dried and purified using alumina columns. All reactions were monitored by thin-layer chromatography (TLC) using a Merck TCL silica gel 60 F254. NMR spectra were recorded on a JEOL JMS ECS 400 MHz spectrometer (100 MHz for ^{13}C and 128.2 MHz for ^{11}B). The reference used for ^{11}B was a solution of BF_3OEt_2 15% in $CDCl_3$ contained in a coaxial insert, with the reference peak at 0 ppm for ^{11}B. High resolution mass spectroscopy was performed using the CNRS Imaging platform. The melting points were measured using a Stuart SMP10 apparatus. Syntheses of **P-Ester** and **DFB-Ester** compounds have been described in a previous article.[17]

DPB-Ester synthesis. Triphenylborane BPh_3 (0.29 g, 1.20 mmol, 1.10 eq.) was added to a solution of diketone (0.340 g, 1.1 mmol, 1.0 eq.) in anhydrous CH_2Cl_2 (C = 0.12 mol L^{-1}) under argon. The mixture was refluxed overnight, and then the solvent was removed *in vacuo*. The crude product was purified by column chromatography on silica (eluent $CHCl_3$). **DPB-Ester** was isolated as a yellow solid (398 mg, 0.84 mmol, 76% yield).

R_f (50/50 petroleum ether/EtOAc) = 0.71. ^{1}H NMR ($CDCl_3$): δ = 8.18 (m, 6H); 7.59 (d, J = 7.0 Hz, 4H); 7.27 (m, 4H); 7.20 (m, 2H); 7.04 (d, J = 9.2 Hz, 2H); 6.94 (s, 1H); 3.97 (s, 3H); 3.92 (s, 3H). ^{13}C NMR ($CDCl_3$): δ = 183.1; 180.1; 166.1; 165.4; 137.6; 134.5; 131.44; 131.41; 130.0; 128.2; 127.3; 126.7; 125.4; 114.7; 94.2; 55.9; 52.7. ^{11}B NMR δ = −0.90. HRMS (ES+) calculated for $[C_{30}H_{25}BO_5K]^+$ 515.1432, found 515.1423. Mp 220 °C.

X-Ray crystallography

X-ray diffraction data for compound **P-Ester** were collected by using a VENTURE PHOTON100 CMOS Bruker diffractometer with Micro-focus IuS source Mo Kα radiation. Crystals were mounted on a CryoLoop (Hampton Research) with Paratone-N (Hampton Research) as a cryoprotectant and then flashfrozen in a nitrogen-gas stream at 100 K. The temperature of the crystal was maintained at the selected value by means of an N-Helix series Cryostream cooling device within an accuracy of ±1 K. The data were corrected for Lorentz polarization, and absorption effects. The structures were solved by direct methods using SHELXS-97 [18] and refined against F2 by full-matrix least-squares techniques using SHELXL-2017 [19] with anisotropic displacement parameters for all non-hydrogen atoms. Hydrogen atoms were located on a difference Fourier map and introduced into the calculations as a riding model with isotropic thermal parameters. All calculations were performed by using the Crystal Structure crystallographic software package WINGX.[20] The crystal data collection and refinement parameters are given in Table S1.†

CCDC 1823426† contains the supplementary crystallographic data for this paper.

Calculations

Calculations were performed using the hybrid B3LYP functional, as implemented in Gaussian 09 software package.[21] For geometry optimization, a 6-31G(d) basis set was used. All minima were verified *via* a calculation of vibrational frequencies, ensuring that no imaginary frequencies were present. TD-DFT calculations were performed using a 6-311+G(d,p) basis set and solvent effects were modelled using the IEF-PCM model.

Spectroscopic measurements

Absorption spectra were recorded on a double beam CARY 100 spectrophotometer. Steady-state emission spectra in solution were obtained on a Fluoromax-3 or Fluorolog-3-221 spectrofluorimeter from Horiba Jobin–Yvon. The signal was collected at 90° with respect to the excitation beam. Fluorescence spectra of a thin film deposited on paper were recorded on the Fluorolog-3-221 spectrofluorimeter, and the signal was collected at 22.5° with respect to the excitation beam (front-face mode). Fluorescence quantum yields in a diluted solution were determined using quinine sulfate as a reference, dissolved in a solution of 0.5 M H_2SO_4 (literature Φ_F = 0.54). All spectra were recorded on aerated solutions, unless specified. Fluorescence quantum yields in the solid state were obtained using a Fluorolog-3-221 integrating sphere, with a Horiba

Jobin–Yvon acquisition and analysis software. Fluorescence decay curves were obtained by the time-correlated single-photon counting (TCSPC) method with femtosecond laser excitation composed of a Titanium-Sapphire laser (Tsunami, Spectra-Physics) pumped by a doubled Nd:YVO laser (Millennia Xs, Spectra-Physics). Light pulses at 780 nm from the oscillator were selected by an acousto-optic crystal at a repetition rate of 4 MHz, and then doubled at 390 nm by a non-linear crystal. Fluorescence photons were detected at 90° through a monochromator and a polarizer at the magic angle by means of a Hamamatsu MCP R3809U photomultiplier, connected to a SPC-630 TCSPC module from Becker &Hickl. The fluorescence data were analyzed using the Globals software package developed at the Laboratory for Fluorescence Dynamics at the University of Illinois at Urbana–Champaign, which includes reconvolution analysis and global nonlinear least-squares minimization method.

Results and discussion

Synthesis and photophysical properties in solution

The target **DPB** compound was prepared by the reaction of the diketone precursors, whose synthesis is described elsewhere,[17] with triphenylborane in refluxing dichloromethane, following an established procedure[16] (Scheme 1). It was isolated with 76% yield as a yellow solid after purification by chromatography on silica gel.

The photophysical properties of the **P-Ester** compound and its diphenyl-boron complex **DPB-Ester** were studied in a THF solution (Fig. 2) and compared with those of the corresponding difluoro-boron complex **DFB-Ester** (Table 1). Compared to the free diketone **P-Ester**, complexation by a boron moiety induces a red-shift of the absorption spectrum which is more important for **DPB-Ester** (3330 cm^{-1}) than for **DFB-Ester** (2270 cm^{-1}). The molar absorption coefficient of **DPB-Ester** (21 000 L mol^{-1} cm^{-1}) is smaller than that of free diketone **P-Ester** (31 000 L mol^{-1} cm^{-1}) which in turn is smaller than that of the **DFB-Ester** complex (46 000 L mol^{-1} cm^{-1}).

Complexation also induces a red-shift of the fluorescence emission spectra. The fluorescence emission maximum of **DPB-Ester** is very similar to that of **DFB-Ester**, implying a limited Stokes shift and a significant overlap between the absorption and emission bands for **DPB-Ester**. This smaller Stokes shift for **DPB-Ester** suggests that in this compound, the excited state has a lower charge transfer character than the

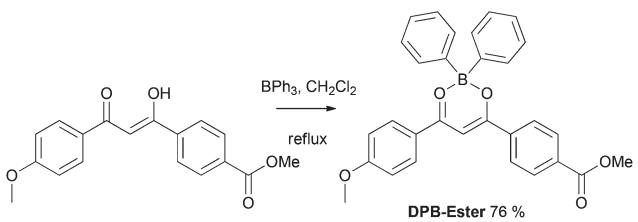

Scheme 1 Synthesis of the **DPB-Ester** compound.

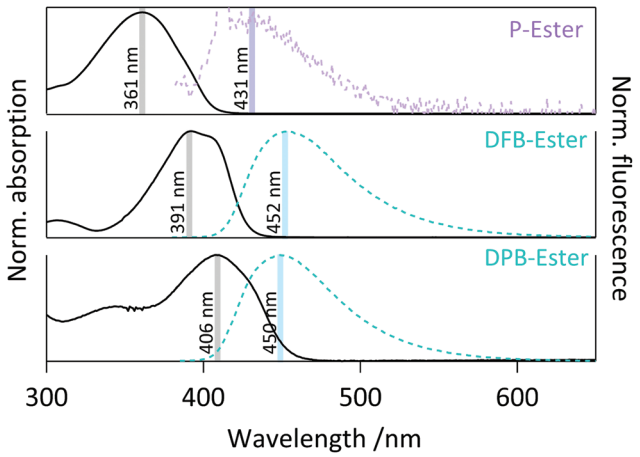

Fig. 2 Absorption (in black) and fluorescence emission (in coloured lines), of the **P-Ester**, **DFB-Ester** and **DPB-Ester** compounds in THF solution. λ_{exc} = 390 nm.

Table 1 Photophysical properties of the **P-Ester** molecule and its boron complexes **DPB-Ester** and **DFB-Ester** in THF

	λ_{max} (abs)/nm	λ_{max} (em)/nm	ε/L mol^{-1} cm^{-1}	Φ_F	τ/ns
P-Ester	361	431	31 000	$<2 \times 10^{-3}$	⟨0.19⟩
DFB-Ester	391	452	46 000	0.85	2.37
DPB-Ester	406	450	21 000	0.01	⟨0.92⟩

P-Ester and **DFB-Ester** compounds. The fluorescence quantum yield of the **P-Ester** compound is very low ($\Phi < 2 \times 10^{-3}$, associated with very short decay $\langle\tau\rangle$ = 0.19 ns) and only slightly increases upon complexation by a boron-diphenyl moiety (Φ = 0.01 for the **DPB-Ester**, with an average fluorescence lifetime $\langle\tau\rangle$ = 0.92 ns) indicating that not only the presence but also the nature of the chelating boron moiety has a crucial influence on the fluorescence properties of these diketonate complexes. The bathochromic shifts in absorption and emission as well as the fluorescence enhancement upon complexation by a boron-difluoride moiety are fully consistent with a previous report by Fraser *et al.* on dinaphthoylmethane β-diketones.[11] In contrast, the weak fluorescence emission of the **DPB-Ester** molecule strongly differs from the bright emission described by Zhang *et al.* for a related diphenylboron diketonate complex.[22]

DFT calculations

DFT calculations were performed on the **P-Ester** and the **DPB-Ester** compounds and compared with the calculations on **DFB-Ester**.[17] Geometry optimization shows that the **P-Ester** compound adopts a slightly twisted geometry (Fig. 3): the methoxyphenyl and the *p*-methylbenzoate rings form dihedral angles of 9.6° and 15.8° respectively with the dioxaborinine ring. Complexation of the diketone by a boron diphenyl group does not significantly change the conformation of the diketone, in a similar fashion to that observed for **DFB-Ester**, with a dihedral angle of −1.5° (resp. 17.9°) between the meth-

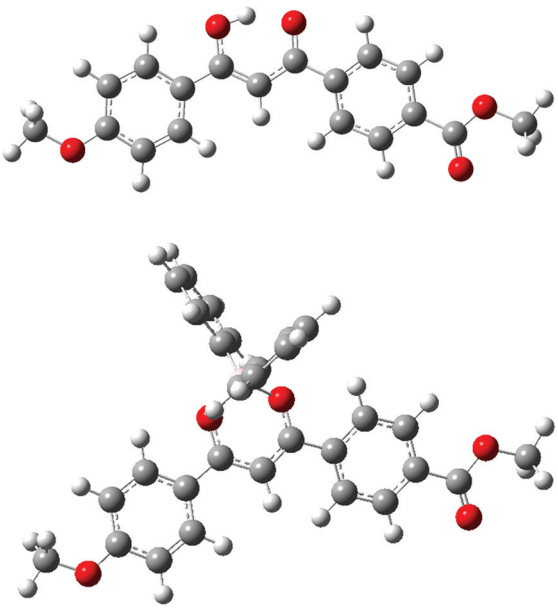

Fig. 3 Geometry optimization (DFT B3LYP/6-31G(d)) for compounds **P-Ester** (top) and **DPB-Ester** (bottom).

oxyphenyl (resp. the *p*-methylbenzoate) ring and the dioxaborinine ring in the **DPB-Ester** compound. The geometry around the boron atom is tetrahedral.

TD-DFT calculations were then performed, using an implicit IEF-PCM solvent model. The position of the first Franck–Condon transition was compared with the maximum of the first absorption band in the experimental spectra. For both **DPB-Ester** and **P-Ester** good agreement was obtained (Table 2). For **DPB-Ester** the first vertical transition has a weak oscillator strength and is followed by a more intense transition (Table 2), while for **P-Ester** and **DFB-Ester** the first vertical transition shows a high oscillator strength, corresponding to the first absorption band. For **P-Ester**, the first transition only implies a HOMO → LUMO transition which is of the π → π* type with a charge transfer character. The second transition implies a HOMO−2 → LUMO, a HOMO−4 → LUMO and a HOMO−6 → LUMO transition: Natural Transition Orbitals (NTO)[23] were computed (Table 3) and it was revealed that for this transition the hole is mainly located on a non-bonding orbital while the electron is located on a π*-type orbital. For **DPB-Ester**, the first transition involves only the HOMO−1 and LUMO orbitals, which are spatially separated, HOMO−1 being localized on the diphenyl-boron moiety and the LUMO being of π*-type, on the diketone.‡ The second transition implies a HOMO → LUMO transition and a HOMO−5 → LUMO transition. Again, NTO analysis demonstrates that this transition is of the π → π* type with a weaker charge transfer character than in the case of **P-Ester**. This weaker charge transfer character is in good agreement with the smaller Stokes shift observed experimentally. By comparison, the first transition computed for **DFB-Ester** is also of the π → π* type with a charge transfer character which only implies a HOMO → LUMO transition, and is very similar to the first transition observed in **P-Ester**. The analysis of the orbitals involved in the first Frank–Condon transition suggests the existence of a low-energy excited-state for **DPB-Ester** that can be reached from the ground-state by a weakly allowed transition (low oscillator strength). This excited-state could be involved in non-radiative deactivation

Table 2 Experimental and computed absorption wavelengths

	λ_{max} (abs)/nm experimental	1st computed transition/nm (oscillator strength *f*)	2nd computed transition/nm (oscillator strength *f*)
P-Ester	362	386 (*f* = 0.815)	333 (*f* = 0.004)
DFB-Ester	392	399 (*f* = 1.01)	324 (*f* = 0.010)
DPB-Ester	409	415 (*f* = 0.015)	406 (*f* = 0.698)

Table 3 Natural transition orbitals computed for the first and second vertical absorption transitions of **P-Ester**, **DFB-Ester** and **DPB-Ester** compounds

Hole	Electron
P-Ester transition 1 (386 nm)[a]	
P-Ester transition 2 (333 nm)	
DFB-Ester, transition 1 (399 nm)[a]	
DPB-Ester, transition 1 (415 nm)[a]	
DPB-Ester, transition 2 (406 nm)	

[a] These transitions involve only one orbital for the hole and one for the electron; consequently, the orbitals involved are directly represented, without the need for NTO computation.

‡ Despite the spatially separated orbitals, the fluorescence emission spectra are identical for aerated and degassed solutions, which indicates the absence of delayed fluorescence in this compound.

processes that could partly explain the low fluorescence quantum yield observed in solution. In contrast, for the brightly fluorescent **DFB-Ester**, only one allowed transition is computed in the main absorption band. For **P-Ester**, the first transition computed is also allowed; however free rotations within the diketone moiety can explain fast non-radiative deactivation and low fluorescence quantum yield in solution. Chujo *et al.* performed DFT calculations on a related diphenylboron β-diketonate complex and its di-(pentafluorophenyl)-boron analog.[24] They arrived at similar conclusions from the analysis of the orbitals: a π-type HOMO localized on the diketone seems to be correlated with a bright fluorescence in solution and may be favored by electron withdrawing substituents located on the boron chelating group, such as fluorine or pentafluorophenyl.

Structure determination

Crystallization tests were performed for the three compounds.

Single crystals of the **P-Ester** compound suitable for X-ray diffraction were isolated by slow evaporation of a mixture of ethyl acetate and petroleum ether (1 : 1). Unfortunately, suitable crystals could not be obtained for **DPB-Ester**, although DSC analysis, which shows a fusion endotherm at 220 °C (see the ESI†), indicates that the powder isolated from the synthesis is partially crystalline. As described previously,[17] two different polymorphs were isolated for **DFB-Ester**. **P-Ester** crystallizes in a face-centered cubic system, composed of 8 molecules per cells. The precursor is slightly distorted, with both phenyl moieties, namely *p*-methoxyphenyl and *p*-methylbenzoate, forming angles of 15.79° and 10.36° with the dioxaborinine ring, respectively (Fig. 4). This corresponds to a geometry similar to the one computed in the gas phase. Molecules are associated in pairs. In each pair the molecules are parallel but the substituents (methoxy and methyl) are on opposite sides (Fig. 4B and C). The molecules within one pair are separated by 3.693 Å (distance measured between the centroids) with a partial overlap of the phenyl moieties.

The pair system was also found for **DFB-Ester** but, in contrast to **P-Ester**, the molecules were always antiparallel.[17] **DFB-Ester** also displayed a polymorphic behaviour which was not revealed for the precursor. Furthermore, for the two polymorphs of **DFB-Ester**, distances between centroids within the pairs were shorter (3.41 Å in the green-emitting crystal and 3.52 Å in the yellow-emitting crystal respectively)[17] which indicates stronger intermolecular interactions in the **DFB-Ester** crystals.

Solid-state fluorescence and mechanofluorochromism

In the case of **P-Ester** the transition from the THF solution to the micro-crystalline solid-state comes along with a modest bathochromic shift of the emission (from 431 nm to 450 nm; 1080 cm^{-1}) and an enhancement of the fluorescence quantum yield (from 0.002 to 0.025), together with longer fluorescence decay ($\langle\tau\rangle$ = 2.41 ns at 450 nm; see the ESI†). In the solid state, the deactivation processes by rotational motion are limited compared to that in solution, which explains the fluorescence

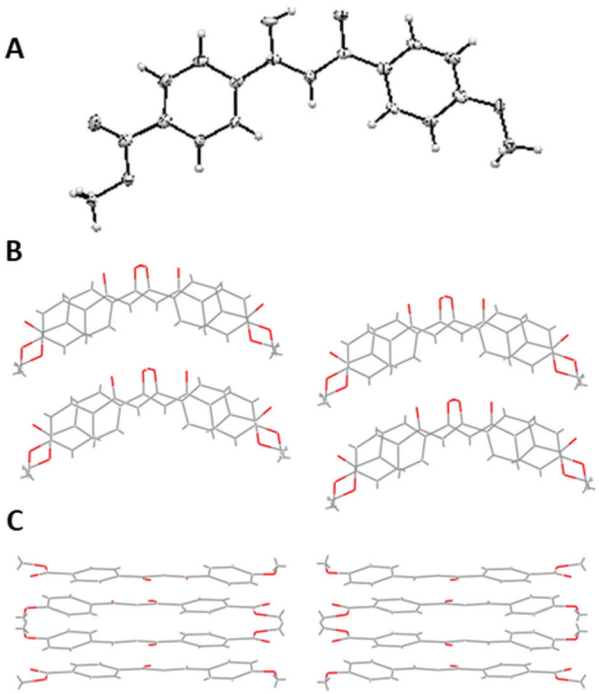

Fig. 4 ORTEP diagram of compound **P-Ester** (A), and molecular packing in crystal: view along the b axis (B) and along the c axis (C).

enhancement. The isolated powder displays a weak blue emission. For **DPB-Ester** the transition to the solid-state does not bring any modification of the fluorescence quantum yield which stays around 0.01. Here, unfortunately, the AIEE phenomenon was not observed, which is consistent with the fact that the molecule was already rigidified by complexation with the boron diphenyl moiety. Nevertheless, a strong bathochromic shift of 82 nm (3430 cm^{-1}) can be underlined with a new maximum of the fluorescence centred at 532 nm. By comparison, for **DFB-Ester** going from the THF solution to the solid-state also induces a bathochromic shift of the emission (from 452 nm for the solution to 494 nm for a crystalline thin film; 1880 cm^{-1}) but in this case a partial quenching of the fluorescence emission is observed, with quantum yields decreasing from 0.85 for the THF solution to 0.32 for the crystalline thin film.[17] Overall, the complexation of the diketonate by the boron chelating complex seems to lead to an increase of the bathochromic shift when going from the solution to the solid-state.

The mechanofluorochromic behaviour of the three different compounds was then compared (Fig. 5). The powders, isolated from synthesis, were smeared for 30 seconds in an agate mortar. Similar to **DFB-Ester**, the precursor **P-Ester** revealed itself to be mechanofluorochromic with a 47 nm bathochromic shift (from 450 nm to 497 nm; 2100 cm^{-1}) together with a significant broadening of the emission spectrum. Excitation spectra revealed comparable shapes for the different phases (see the ESI†). In the case of **DPB-Ester**, no mechano-induced change of emission was observed. At first sight, these results seem to differ greatly from the system described by Zhang

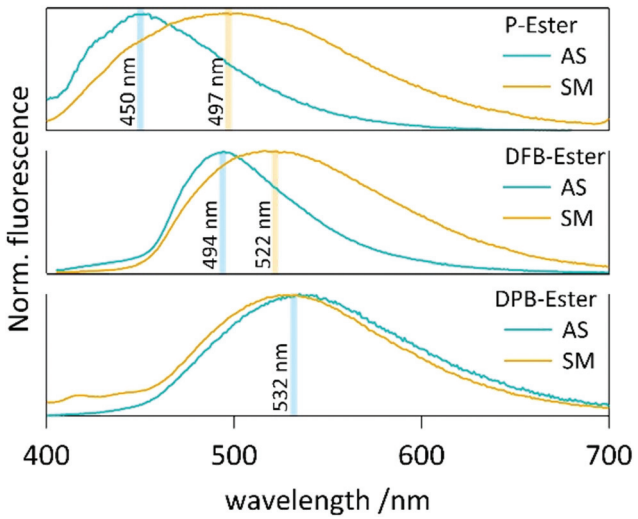

Fig. 5 Solid-state emission spectra of the crystalline powders isolated from synthesis (as synthesized – AS) and the powders after grinding in a mortar (smeared – SM).

et al. where the diphenylboron complex was not only mechanofluorochromic but also showed a distinct fluorescence response to distinct types of mechanical stimuli (grinding or hydrostatic pressure).[16] However, it is worth noting that Zhang *et al.* describe a sensitivity to hydrostatic pressure in the GPa range, as well as the apparition of an hypsochromic shift of the fluorescence when crystals are "smashed" but that the fluorescence of their diphenylboron complex does not change significantly upon grinding the crystals in a mortar. In the literature, the mechanofluorochromic response of the difluoroboron β-diketonate complexes is attributed to easier excimer formation in the amorphous phase, allowed by a higher conformational freedom.[25] Our data, both on the solid-state fluorescence properties and on the geometry optimization by DFT, together with a careful examination of the data published by Zhang *et al.* suggest that the steric hindrance induced by the bulkydiphenylboron group may prevent this excimer formation, thus suppressing the sensitivity of this class of compounds to the shearing stress induced upon grinding.

Conclusions

In conclusion a diphenyl-boron β-diketonate complex **DPB-Ester** was synthesized and its photophysical properties were compared in solution and in the solid state to those of its parent free diketone **P-Ester** and to those of the corresponding difluoro-boron β-diketonate complex **DFB-Ester**. This series of compounds show clearly distinct properties. **DFB-Ester** is strongly fluorescent in solution, and remains fluorescent in the solid-state despite a lower quantum yield. **P-Ester** is very weakly fluorescent in solution and displays significant AIEE in the crystalline state, which can be explained by the rigidification of the molecule in the crystal lattice. **DPB-Ester** exhibits a weak fluorescence, both in solution and in the solid-state. TD-DFT calculations reveal that **DPB-Ester** possesses a low-lying excited state that could play a role in the efficient non-radiative deactivation processes occurring in these two compounds.

For both **P-Ester** and **DFB-Ester**, a mechanofluorochromic response was observed upon grinding the crystalline powder in a mortar, whereas for **DPB-Ester** no fluorescence emission change is observed. The steric hindrance induced by the bulky diphenyl-boron chelating group may prevent excimer formation in the amorphous phase for the **DPB-Ester** whereas this has been shown to occur at the origin of the mechanofluorochromic shift for **DFB-Ester**[17] and for related compounds.[5,25] Thus, comparison of our results with the literature indicates that diphenyl-boron β-diketonate complexes could be interesting to obtain compounds sensitive to hydrostatic pressure and not to shearing stress (obtained by grinding), provided they are highly fluorescent. Complexation of more electron-rich β-diketones with a diphenyl-boron group may be a promising way to design such fluorescent complexes.

Conflicts of interest

There are no conflicts to declare.

Acknowledgements

This project has received funding from the European Research Council (ERC) under the European Union's Horizon 2020 research and innovation programme (grant agreement No 715757 MECHANO-FLUO to C. A.) and from the IDEX Paris-Saclay (Ph. D. fellowship to M. L.).

Notes and references

1 J. Xu and Z. Chi, *Mechanochromic Fluorescent Materials: Phenomena, Materials and Applications*, The Royal Society of Chemistry, 2014.
2 P. Xue, J. Ding, P. Wang and R. Lu, Recent progress in the mechanochromism of phosphorescent organic molecules and metal complexes, *J. Mater. Chem. C*, 2016, **4**, 6688–6706.
3 Y. Sagara, S. Yamane, M. Mitani, C. Weder and T. Kato, Mechanoresponsive Luminescent Molecular Assemblies: An Emerging Class of Materials, *Adv. Mater.*, 2016, **28**, 1073–1095.
4 C. Calvino, L. Neumann, C. Weder and S. Schrettl, Approaches to polymeric mechanochromic materials, *J. Polym. Sci., Part A: Polym. Chem.*, 2017, **55**, 640–652.
5 G. Zhang, J. Lu, M. Sabat and C. L. Fraser, Polymorphism and reversible mechanochromic luminescence for solid-state difluoroboron avobenzone, *J. Am. Chem. Soc.*, 2010, **132**, 2160–2162.
6 T. Sagawa, F. Ito, A. Sakai, Y. Ogata, K. Tanaka and H. Ikeda, Substituent-dependent backward reaction in

mechanofluorochromism of dibenzoylmethanatoboron difluoride derivatives, *Photochem. Photobiol. Sci.*, 2016, **15**, 420–430.

7 A. Sakai, E. Ohta, Y. Yoshimoto, M. Tanaka, Y. Matsui, K. Mizuno and H. Ikeda, New Fluorescence Domain "Excited Multimer" Formed upon Photoexcitation of Continuously Stacked Diaroylmethanatoboron Difluoride Molecules with Fused pi-Orbitals in Crystals, *Chem. – Eur. J.*, 2015, **21**, 18128–18137.

8 P. Galer, R. C. Korosec, M. Vidmar and B. Sket, Crystal structures and emission properties of the BF(2) complex 1-phenyl-3-(3,5-dimethoxyphenyl)-propane-1,3-dione: multiple chromisms, aggregation- or crystallization-induced emission, and the self-assembly effect, *J. Am. Chem. Soc.*, 2014, **136**, 7383–7394.

9 W. A. Morris, T. Liu and C. L. Fraser, Mechanochromic luminescence of halide-substituted difluoroboron β-diketonate dyes, *J. Mater. Chem. C*, 2015, **3**, 352–363.

10 S. Xu, R. E. Evans, T. Liu, G. Zhang, J. N. Demas, C. O. Trindle and C. L. Fraser, Aromatic difluoroboron beta-diketonate complexes: effects of pi-conjugation and media on optical properties, *Inorg. Chem.*, 2013, **52**, 3597–3610.

11 T. Butler, W. A. Morris, J. Samonina-Kosicka and C. L. Fraser, Mechanochromic Luminescence and Aggregation Induced Emission of Dinaphthoylmethane beta-Diketones and Their Boronated Counterparts, *ACS Appl. Mater. Interfaces*, 2016, **8**, 1242–1251.

12 W. A. Morris, T. Butler, M. Kolpaczynska and C. L. Fraser, Stimuli Responsive Furan and Thiophene Substituted Difluoroboron beta-Diketonate Materials, *Mater. Chem. Front.*, 2017, **1**, 158–166.

13 F. Wang, C. A. DeRosa, M. L. Daly, D. Song, M. Sabat and C. L. Fraser, Multi-stimuli responsive luminescent azepane-substituted β-diketones and difluoroboron complexes, *Mater. Chem. Front.*, 2017, **1**, 1866–1874.

14 T. Butler, F. Wang, M. Sabat and C. L. Fraser, Controlling solid-state optical properties of stimuli responsive dimethylamino-substituted dibenzoylmethane materials, *Mater. Chem. Front.*, 2017, **1**, 1804–1817.

15 J. Hu, Z. He, Z. Wang, X. Li, J. You and G. Gao, A simple approach to aggregation-induced emission in difluoroboron dibenzoylmethane derivatives, *Tetrahedron Lett.*, 2013, **54**, 4167–4170.

16 L. Wang, K. Wang, B. Zou, K. Ye, H. Zhang and Y. Wang, Luminescent chromism of boron diketonate crystals: distinct responses to different stresses, *Adv. Mater.*, 2015, **27**, 2918–2922.

17 M. Louis, A. Brosseau, R. Guillot, F. Ito, C. Allain and R. Métivier, Polymorphism, Mechanofluorochromism, and Photophysical Characterization of a Carbonyl Substituted Difluoroboron-β-Diketone Derivative, *J. Phys. Chem. C*, 2017, **121**, 15897–15907.

18 G. M. Sheldrick, *SHELXS-97, Program for Crystal Structure Solution*, University of Göttingen, Göttingen, Germany, 1997.

19 G. M. Sheldrick, *Acta Crystallogr., Sect. A: Found. Crystallogr.*, 2008, **64**, 112–122.

20 L. J. Farrugia, *J. Appl. Crystallogr.*, 1999, **32**, 837.

21 M. J. Frisch, G. W. Trucks, H. B. Schlegel, G. E. Scuseria, M. A. Robb, J. R. Cheeseman, G. Scalmani, V. Barone, G. A. Petersson, H. Nakatsuji, *et al.*, *Gaussian 09*, Gaussian, Inc., Wallington CT, 2009.

22 L. Wang, Z. Zhang, X. Cheng, K. Ye, F. Li, Y. Wang and H. Zhang, Red emissive diarylboron diketonate crystals: aggregation-induced color change and amplified spontaneous emission, *J. Mater. Chem. C*, 2015, **3**, 499–505.

23 R. L. Martin, Natural transition orbitals, *J. Chem. Phys.*, 2003, **118**, 4775–4777.

24 A. Nagai, K. Kokado, Y. Nagata, M. Arita and Y. Chujo, Highly intense fluorescent diarylboron diketonate, *J. Org. Chem.*, 2008, **73**, 8605–8607.

25 G. Zhang, J. P. Singer, S. E. Kooi, R. E. Evans, E. L. Thomas and C. L. Fraser, Reversible solid-state mechanochromic fluorescence from a boron lipid dye, *J. Mater. Chem.*, 2011, **21**, 8295.